Orientationally-Selected Two-Dimensional ESEEM Spectroscopy of the Rieske-Type Iron−Sulfur Cluster in 2,4,5-Trichlorophenoxyacetate Monooxygenase from *Burkholderia cepacia* AC1100

Sergei A. Dikanov,*,†,‡ Luying Xun,§ Adrienne B. Karpiel,† Alexei M. Tyryshkin,‡ and Michael K. Bowman†

Contribution from Macromolecular Structure and Dynamics, Environmental Molecular Sciences Laboratory, Pacific Northwest National Laboratory, Richland, Washington 99352, the Institute of Chemical Kinetics and Combustion, Russian Academy of Sciences, Novosibirsk 630090, Russia, and the Department of Microbiology and Immunology, Washington State University at Tri-Cities, Richland, Washington 99352

Received March 11, 1996[⊗]

Abstract: *Burkholderia cepacia* AC1100 is able to use the chlorinated compound 2,4,5-trichlorophenoxyacetic acid (2,4,5-T) as the sole source of carbon and energy. CW EPR and one-dimensional ESEEM spectroscopy studies performed earlier indicate the presence of a Rieske-type [2Fe-2S] cluster with two coordinated histidine residues in 2,4,5-T monooxygenase from *B. cepacia*. This paper describes the application of two-dimensional ESEEM (called HYSCORE) spectroscopy for further characterization of the nitrogens surrounding the reduced Rieske-type cluster. The HYSCORE spectra measured at field positions in the neighborhood of the principal directions of the **g** tensor contain major contributions from cross-peaks correlating the two double-quantum transitions from each histidine nitrogen. These allow the estimation of the diagonal components of the hyperfine tensors along the principal axes of the **g** tensor: 4.05, 3.88, and 4.01 MHz (N1) and 4.71, 5.07, and 5.02 MHz (N2). Other spectral features from the histidine nitrogens usually have a much weaker intensity and are occasionally observed in the spectra. HYSCORE measurements have been also performed with the reduced [2Fe-2S] plant ferredoxin-type cluster with four cysteine ligands in a ferredoxin from *Porphira umbilicalis*, and spectral features produced by the peptide nitrogen are observed. Similar features also appear in the HYSCORE spectra of the Rieske cluster. Systematic differences are observed between 2,4,5-T monooxygenase and published results from related benzene and phthalate dioxygenases that may reflect structural and functional differences in histidine ligation and the nitrogens of nearby amino acids in Rieske-type [2Fe-2S] clusters.

Introduction

Burkholderia cepacia AC1100 is able to use the persistent chlorinated herbicide 2,4,5-trichlorophenoxyacetate (2,4,5-T) as the sole source of carbon and energy.[1] This organism was previously assigned to the genus *Pseudomonas*. The initial step in the biodegradation of 2,4,5-T by *B. cepacia* AC1100 is its conversion to 2,4,5-trichlorophenol (2,4,5-TCP). A multiple-component oxygenase is responsible for the conversion of 2,4,5-T to 2,4,5-TCP. The genes encoding the oxygenase component have been cloned and sequenced. The oxygenase component of the enzyme has also been purified and characterized from AC1100.[1b] The oxygenase component has a native molecular weight of 140 000, and it is composed of two 49 kDa α-subunits and two 24 kDa β-subunits.

The deduced amino acid sequences of α- and β-subunits show homology to the α- and β-subunits of other multicomponent aromatic dioxygenases. The α-subunit has two conserved cysteine−histidine pairs at identical positions (Cys-X-His-17 amino acids-Cys-X-X-His) as in related α-subunits. This motif also occurs in the so-called Rieske protein isolated from the ubiquinol−cytochrome *c* oxidoreductase of bovine heart mitochondria.[2]

Conclusive determination of the ligands in the Rieske-type cluster was obtained by application of the high-resolution EPR techniques of electron-nuclear double resonance (ENDOR) and electron spin-echo envelope modulation (ESEEM) spectroscopies. X- and Q-band ENDOR studies of the reduced Rieske-type cluster in phthalate dioxygenase from *B. cepacia*[3] and in ubiquinol−cytochrome c_2 oxidoreductase from *Rhodobactor capsulatus*[4] established that two histidine ligands are coordinated to one iron in place of two cysteines in the plant ferredoxins. The ESEEM experiments performed on the reduced Rieske clusters in the cytochrome b_6 *f* complex of spinach chloroplast, cytochrome bc_1 complexes of *Rhodospirillum rubrum*, *Rhodobacter sphaeroides* R-26, and bovine heart mitochrondria,[5] in complex III of bovine heart mitochrondrial membranes,[6] and benzene 1,2-dioxygenase from *Pseudomonas*

† Pacific Northwest National Laboratory.
‡ Russian Academy of Sciences.
§ Washington State University at Tri-Cities.
⊗ Abstract published in *Advance ACS Abstracts,* August 15, 1996.

(1) (a) Danagan, C. E.; Ye, R. W.; Daubaras, D. L.; Xun, L.; Charkabarty, A. M. *Appl. Environ. Microbiol.* **1994**, *60*, 4100. (b) Xun, L.; Wagnon, K. B. *Appl. Environ. Microbiol.* **1995**, *61*, 3499.

(2) (a) Cammack, R. In *Advances in Inorganic Chemistry. Iron-Sulfur Proteins*; Cammack, R., Sykes, A. G., Eds.; Academic Press: San Diego, 1992; Vol. 38, p 281. (b) Mason, J. R.; Cammack, R. *Annu. Rev. Microbiol.* **1992**, *46*, 277.

(3) Gurbiel, R. J.; Batie, C. J.; Sivaraja, M.; True, A. E.; Fee, J. A.; Hoffman, B. M.; Ballou, D. P. *Biochemistry* **1989**, *28*, 4861.

(4) Gurbiel, R. J.; Ohnishi, T.; Robertson, D. E.; Daldal, F.; Hoffman, B. M. *Biochemistry* **1991**, *30*, 11579.

(5) Britt, R. D.; Sauer, K.; Klein, M. P.; Knaff, D. B.; Kriauciunas, A.; Yu, C. A.; Yu, L.; Malkin, R. *Biochemistry* **1991**, *30*, 1892.

S0002-7863(96)00781-0 CCC: $12.00

putida[7] all show two-coordinated ^{14}N histidine nitrogens with hyperfine constants between 3.6−4.5 and 4.6−5.5 MHz. In contrast, ESEEM and ENDOR investigations of plant ferredoxin-type [2Fe-2S] clusters with four cysteine ligands show only interaction with nitrogens having a maximum hyperfine coupling of ∼1 MHz.[8] We were able to assign this coupling to a nitrogen in the peptide backbone.[8f]

We recently[9] confirmed the presence of a Rieske-type [2Fe-2S] cluster with two coordinated nitrogens in 2,4,5-T monooxygenase from *B. cepacia* AC1100 similar to those in other multicomponent oxygenases, ferredoxins, and mitochondrial proteins. The present work reports a more detailed investigation of the nitrogens surrounding the Rieske cluster in 2,4,5-T monooxygenase using the advanced, two-dimensional pulsed EPR technique of HYSCORE spectroscopy. We first discuss some of the general features of the HYSCORE spectra for nitrogens in orientationally-disordered systems and then present the results from 2,4,5-T monooxygenase and discuss its analysis before considering the differences between the related Rieske-type clusters.

Experimental Section

The oxygenase was isolated and purified as described earlier.[1] The EPR measurements were performed with samples containing about 200 μM protein, 50 mM tris−HCl (pH 7.6), and 50% by volume glycerol. The protein was chemically reduced by addition of an aqueous solution of 0.01 M sodium dithionite ($Na_2S_2O_4$) in slight excess to the protein solution under anaerobic conditions.

EPR Experiments. Pulsed EPR experiments were performed with an X-band Bruker ESP-380 spectrometer with a dielectric low-Q resonator. The length of a $\pi/2$ pulse was nominally 16 ns. Four-step phase cycles, $+(0,0,0)$, $-(0,\pi,0)$, $-(\pi,0,0)$ $+(\pi,\pi,0)$ in the three-pulse sequence[10] and $+(0,0,0,0)$, $-(0,0,0,\pi)$, $+(0,0,\pi,0)$, $-(0,0,\pi,\pi)$[11] in the four-pulse HYSCORE sequence,[12] were used to eliminate unwanted features from echo envelopes. An Oxford Instruments CF935 helium cryostat was used for temperature variation and control. Spectral processing of three- and four-pulse two-dimensional ESEEM patterns was performed using Bruker WIN-EPR software.

HYSCORE Spectroscopy of ^{14}N Nuclei. When the paramagnetic metal in the active site of a metalloprotein is ligated by even a few nitrogens with different hyperfine and quadrupole couplings, it is often difficult to interpret the one-dimensional (1D) ESEEM spectra due to congestion and overlap of the lines. One fruitful way of simplifying the analysis of complex 1D ESEEM spectra is the use of two-dimensional (2D) techniques. The general advantage of two-dimensional techniques lies in the creation of nondiagonal cross-peaks whose coordinates are nuclear frequencies from opposite electron spin manifolds. Among the 2D techniques, HYSCORE (hyperfine sublevel correlation) spectroscopy is finding increasing application. HYSCORE spectroscopy is based on the four-pulse, two-dimensional ESEEM experiment with a pulse sequence of $\pi/2-\tau-\pi/2-t_1-\pi-t_2-\pi/2-\tau-$echo.[12] The intensity of the inverted echo after the fourth pulse is measured as a function of t_2 and t_1 with constant τ. Such a 2D set of echo envelopes gives, after complex Fourier transformation (FT), a 2D spectrum with equal resolution in each dimension.

The nondiagonal cross-peaks from a nucleus of arbitrary spin evolve according to[13]

$$V(\tau,t_1,t_2) = \sum_{ikmn} A_{ikmn} \exp(-2\pi i \nu_{ik\alpha} t_2) \exp(-2\pi i \nu_{mn\beta} t_1) + B_{ikmn} \exp(-2\pi i \nu_{ik\alpha} t_1) \exp(-2\pi i \nu_{mn\beta} t_2) \quad (1)$$

with

$$A_{ikmn} = \sum_{jl} (M_{kl} M_{li}^{\ddagger} M_{mj}^{\ddagger} M_{jn} M_{im} M_{nk}^{\ddagger}) \{\exp[-2\pi i(\nu_{jk\alpha} + \nu_{ln\beta})\tau] + \exp[2\pi i(\nu_{ji\alpha} + \nu_{lm\beta})\tau]\}$$

$$B_{ikmn} = \sum_{jl} (M_{kl} M_{li}^{\ddagger} M_{mj}^{\ddagger} M_{jn} M_{im} M_{nk}^{\ddagger})^* \{\exp[-2\pi i(\nu_{jk\alpha} + \nu_{ln\beta})\tau] + \exp[2\pi i(\nu_{ji\alpha} + \nu_{lm\beta})\tau]\}$$

The indices i, j, and k number the nuclear levels in the α electron spin manifold and l, m, and n those in the β manifold. M_{kl} is an element of Mims' **M** matrix,[14] giving the EPR transition amplitude from the kth sublevel within the α manifold to the lth sublevel within the β manifold, $\nu_{ik\alpha}$ and $\nu_{mn\beta}$ are the frequencies of the nuclear transitions between levels i and k in the α and m and n in the β manifold.

The frequency $\nu_{ik\alpha} = -\nu_{ki\alpha}$; thus, a pair of cross-peaks related by taking the negative of both frequencies such as ($\nu_{ik\alpha}$, $\nu_{mn\beta}$) and ($\nu_{ki\alpha}$, $\nu_{nm\beta}$) = ($-\nu_{ik\alpha}$, $-\nu_{mn\beta}$) have intensities that are complex conjugates, $A_{ikmn} = A_{kinm}$* and $B_{ikmn} = B_{kinm}$*. This is a consequence of the fact that the experimental HYSCORE signal is a real instead of a complex quantity. In contrast, cross-peaks differing in the sign of one frequency, ($\nu_{ik\alpha}$, $\nu_{mn\beta}$) and ($\nu_{ki\alpha}$, $\nu_{mn\beta}$), i.e., ($-\nu_{ik\alpha}$, $\nu_{mn\beta}$), are characterized by different amplitudes,

$$A_{ikmn} = \{M_{im} M_{kn}^* \sum_{jl} (M_{kl} M_{il}^* M_{jm}^* M_{jn}) \{\exp[-2\pi i(\nu_{jk\alpha} + \nu_{ln\beta})\tau] + \exp[2\pi i(\nu_{ji\alpha} + \nu_{lm\beta})\tau]\}\} \quad (2)$$

$$A_{kimn} = \{M_{km} M_{in}^* \sum_{jl} (M_{il} M_{kl}^* M_{jm}^* M_{jn}) \{\exp[-2\pi i(\nu_{ji\alpha} + \nu_{ln\beta})\tau] + \exp[2\pi i(\nu_{jk\alpha} + \nu_{lm\beta})\tau]\}\}$$

and similarly for B_{ikmn} and B_{kimn}. The summation in eq 2 runs over the products of the same matrix elements with different phase factors which mainly determine the τ dependence of the cross-peak intensity.

These two types of terms predict another important property of HYSCORE spectroscopy—the sensitivity to the relative signs of frequencies involved in the correlation. Due to such characteristics experimental HYSCORE spectra are usually represented by two quadrants, (+ +) and (+ −), of the 2D FT. The coefficients in eq 2 reveal that the intensities of the peaks with the same frequencies in the (+ +) and (+ −) quadrants behave differently because they depend on the products $M_{im}M_{kn}$* or $M_{km}M_{in}$* of matrix elements describing the four possible transitions between two levels, i and k, and m and n, in each manifold. For the major HYSCORE peaks, one pair of transitions may be considered, in the limit of strong or weak hyperfine, as formally "allowed" and the other pair as "forbidden". The amplitudes of these two types of transitions are sensitive to the relative magnitude of the hyperfine to the nuclear Zeeman and quadrupole interactions. As the hyperfine coupling increases, the strong HYSCORE peaks shift from the (+ +) to the (+ −) quadrant.

For a concrete illustration of the correlation features appearing in orientationally-disordered 2D HYSCORE spectra from a nitrogen ^{14}N

(6) Shergill, J. K.; Cammack, R. *Biochim. Biophys. Acta* **1994**, *1185*, 35.
(7) Shergill, J. K.; Joannou, C. L.; Mason, J. R.; Cammack, R. *Biochemistry* **1995**, *34*, 16533.
(8) (a) Cammack, R.; Chapman, A.; McCracken, J.; Cornelius, J. B.; Peisach, J.; Weiner, J. H. *Biochim. Biophys. Acta* **1988**, *956*, 307. (b) Cammack, R.; Chapman, A.; McCracken, J.; Peisach, J. *J. Chem. Soc., Faraday Trans.* **1991**, *87*, 3203. (c) Houseman, A. L. P.; Oh, B.-H. Kennedy, M. C.; Fan, C.; Werst, M. M.; Beinert, H.; Markley, J. L.; Hoffman, B. M. *Biochemistry* **1992**, *31*, 2073. (d) Shergill, J. K.; Cammack, R.; Weiner, J. H. *J. Chem. Soc., Faraday Trans.* **1991**, *87*, 3199. (e) Shergill, J. K.; Cammack, R. *Biochim. Biophys. Acta* **1994**, *1185*, 43. (f) Dikanov, S. A.; Tyryshkin, A. M.; Felli, I.; Reijerse, E. J.; Hüttermann, J. *J. Magn. Reson., Ser. B* **1995**, *108*, 99.
(9) Dikanov, S. A.; Davydov, R. M.; Xun, L.; Bowman, M. K. *J. Magn. Reson., Ser. B*, in press.
(10) Fauth, J.-M.; Schweiger, A.; Braunschweiler, L.; Forrer, J.; Ernst, R. R. *J. Magn. Reson.* **1986**, *66*, 74.
(11) Gemperle, C.; Aebli, G.; Schweiger, A.; Ernst, R. R. *J. Magn. Reson.* **1990**, *88*, 241.
(12) Höfer, P.; Grupp, A.; Nebenführ, H.; Mehring, M. *Chem. Phys. Lett.* **1986**, *132*, 279.
(13) (a) Shane, J. J.; Höfer, P.; Reijerse, E. J.; de Boer, E. *J. Magn. Reson.* **1992**, *99*, 596. (b) Shane, J. J. Electron Spin Echo Envelope Modulation Spectroscopy of Disordered Solids. Ph.D. Thesis, University of Nijmegen, The Netherlands, 1993.
(14) Mims, W. B. *Phys. Rev.* **1972**, *B5*, 2409.

nucleus, let us consider the spin system $S = 1/2$ (in the high-field approximation with an isotropic **g** factor) and $I = 1$ with arbitrary values of isotropic (secular) hyperfine interaction, A, nuclear Zeeman, ν_I, and quadrupole interactions. In this case, the three nuclear resonant frequencies in the two electron spin manifolds are[15]

$$\nu_{ik\alpha(mn\beta)} = (4p_{\alpha(\beta)})^{1/2} \sin[(\gamma_{\alpha(\beta)} + d\pi)/3] \quad (3)$$

$$\gamma_{\alpha(\beta)} = \cos^{-1} C_{\alpha(\beta)}; \quad C_{\alpha(\beta)} = (3/p_{\alpha(\beta)})^{3/2}(q_{\alpha(\beta)}/2)$$

where $p_{\alpha(\beta)} = \nu^2_{\alpha(\beta)} + K^2(3 + \eta^2)$ and $q_{\alpha(\beta)} = \nu_{\alpha(\beta)}{}^2\,[K(3\cos^2\theta - 1 + \eta\sin^2\theta\sin 2\phi)] - 2K^3(1 - \eta^2)$. The azimuthal θ and polar ϕ angles describe the orientation of the external magnetic field in the quadrupole tensor principal axis coordinate system, $\nu_{\alpha(\beta)} = |-\nu_I \pm A/2|$, $K = e^2qQ/4h$ is the quadrupole coupling constant, and η is the asymmetry parameter. In this designation, energy levels (i, k and m, n) are numbered 1, 2, and 3 in the order of their energy and $d = i + k$ or $m + n$.

The cross-peak contour line shape, i.e., the frequency coordinates regardless of intensity, can be described analytically by writing the frequency $\nu_{ik\alpha}$ in terms of the hyperfine and quadrupole coupling parameters and the frequency $\nu_{mn\beta}$ from the opposite manifold. We recently applied such an approach to analyze cross-peak line shapes fron an $I = 1/2$ nuclear spin.[16] With our model for spin $I = 1$, it is possible to obtain the following expression for the parameter[17] which together with eq 3 determines the line shape of the cross-peak correlating *ik* and *mn* transitions from opposite electron spin manifolds:

$$C_{\alpha(\beta)} = (p_{\alpha(\beta)})^{-3/2}\{2^{-1}(\nu_{\alpha(\beta)}/\nu_{\beta(\alpha)})^2(4p_{\beta(\alpha)} - \nu_{mn\beta(ik\alpha)}{}^2)^{1/2} \times (\nu_{mn\beta(ik\alpha)}{}^2 - p_{\beta(\alpha)}) + (3^{3/2})K^3[(\nu_{\alpha(\beta)}/\nu_{\beta(\alpha)})^2 - 1](1 - \eta^2)\} \quad (4)$$

Figure 1 shows the contour line shape of the cross-peaks calculated using eqs 3 and 4 for two limiting cases of hyperfine coupling approximating those in the [2Fe-2S] clusters in Rieske-type proteins and plant-type ferredoxins. In one, the hyperfine coupling $A = 5$ MHz is much larger than both the nitrogen Zeeman frequency $\nu_I = 1.08$ MHz and the quadrupole coupling constant $K = 0.6$ MHz, and models a coordinated histidine nitrogen in the Rieske protein.[3−7,9] In this case, eq 3 yields, in each manifold, the frequency of the double-quantum (**dq**) transition, $\nu_{31\alpha(\beta)} = \nu_{\mathbf{dq}\alpha(\beta)}$, and the two single-quantum (**sq**) transitions, $\nu_{12\alpha(\beta)} = \nu^{(1)}_{\mathbf{sq}\alpha(\beta)}$ and $\nu_{32\alpha(\beta)} = \nu^{(2)}_{\mathbf{sq}\alpha(\beta)}$.

In the second spectrum, the hyperfine coupling $A = 1.1$ MHz is comparable to the Zeeman frequency and the quadrupole constant, $K = 0.81$ MHz, as in the case of a peptide nitrogen in the plant ferredoxin.[8] This set of parameters with $|\nu_I - A/2|/K = 0.65$ corresponds to the case of intermediate deviation from the cancellation condition.[18] Three lines close to the nqr frequencies appear in 1D ESEEM spectra from transitions within the β manifold and one line from the **dq** transition of the α manifold. The frequencies of the α manifold are given by eq 3 as in the previous case. In the β manifold, the three frequencies are $\nu_{31\beta} = \nu_{\mathbf{dq}\beta} \approx \nu_+ = K(3 + \eta)$, $\nu_{21\alpha(\beta)} = \nu^{(2)}_{\mathbf{sq}\beta} \approx \nu_- = K(3 - \eta)$, and $\nu_{32\beta} = \nu^{(1)}_{\mathbf{sq}\beta} \approx \nu_o = 2K\eta$.

The assignment of the different correlation features is shown in Figure 1. There are 18 correlation features from one ^{14}N nitrogen possible in each quadrant. Their location in Figure 1 for the (+ +) quadrant is related by reflection about the ν_1 axis to those in the (+ −) quadrant. The calculation demonstrates in both cases that the most nearly isotropic line shapes belong to features 1 and 1′ correlating **dq** transitions between the extreme nuclear sublevels. This is because their location is mainly determined by the isotropic parameters while the anisotropy contributes in second order only. For the features correlating at least one **sq** transition, the line shape is characterized by a

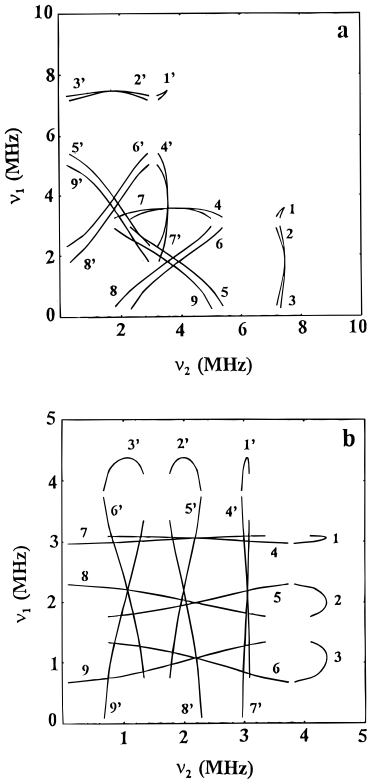

Figure 1. (a) Contour line shape of the cross-peaks from the nitrogen ^{14}N at the hyperfine coupling $A = 5$ MHz, Zeeman frequency $\nu_I = 1.08$ MHz, quadrupole coupling constant $K = 0.6$ MHz, and asymmetry parameter $\eta = 0.5$. (b) The same at $A = 1.1$ MHz, $K = 0.8$ MHz, and $\eta = 0.5$. The numbers indicate the following correlations: 1, 1′, ($\nu_{\mathbf{dq}\beta(\alpha)}$, $\nu_{\mathbf{dq}\alpha(\beta)}$; (2, 2′), ($\nu^{(2)}_{\mathbf{sq}\beta}$, $\nu_{\mathbf{dq}\alpha}$) and ($\nu_{\mathbf{dq}\alpha}$, $\nu^{(2)}_{\mathbf{sq}\beta}$), (3, 3′), ($\nu^{(1)}_{\mathbf{sq}\beta}$, $\nu_{\mathbf{dq}\alpha}$) and ($\nu_{\mathbf{dq}\alpha}$, $\nu^{(1)}_{\mathbf{sq}\beta}$); (4, 4′), ($\nu_{\mathbf{dq}\beta}$, $\nu^{(2)}_{\mathbf{sq}\alpha}$) and ($\nu^{(2)}_{\mathbf{sq}\alpha}$, $\nu_{\mathbf{dq}\beta}$); (5, 5′), ($\nu^{(2)}_{\mathbf{sq}\beta}$, $\nu^{(2)}_{\mathbf{sq}\alpha}$) and ($\nu^{(2)}_{\mathbf{sq}\alpha}$, $\nu^{(2)}_{\mathbf{sq}\beta}$); (6, 6′), ($\nu^{(1)}_{\mathbf{sq}\beta}$, $\nu^{(2)}_{\mathbf{sq}\alpha}$) and ($\nu^{(2)}_{\mathbf{sq}\alpha}$, $\nu^{(1)}_{\mathbf{sq}\beta}$); (7, 7′), ($\nu_{\mathbf{dq}\beta}$, $\nu^{(1)}_{\mathbf{sq}\alpha}$) and ($\nu^{(1)}_{\mathbf{sq}\alpha}$, $\nu_{\mathbf{dq}\beta}$); (8, 8′), ($\nu^{(2)}_{\mathbf{sq}\beta}$, $\nu^{(1)}_{\mathbf{sq}\alpha}$) and ($\nu^{(1)}_{\mathbf{sq}\alpha}$, $\nu^{(2)}_{\mathbf{sq}\beta}$); (9, 9′), ($\nu^{(1)}_{\mathbf{sq}\beta}$, $\nu^{(1)}_{\mathbf{sq}\alpha}$) and ($\nu^{(1)}_{\mathbf{sq}\alpha}$, $\nu^{(1)}_{\mathbf{sq}\beta}$).

significantly larger length which can reach a few megahertz due to the anisotropy of the quadrupole interaction (at the value of $K \approx 0.6-0.8$ MHz the anisotropy of **sq** transitions due to the quadrupole coupling is about 1.5−3.0 MHz). The large number of elongated cross-ridges located in the same area gives the impression of congestion in the HYSCORE spectra. However, we emphasize that these simulations show only the line shape and not the intensity of each cross-ridge. Typically only a subset of these features are visible in the experimental spectra because some of them have negligible intensities while others appear in only one of the two quadrants. For instance, if the energy levels in both manifolds are labeled in accordance with eq 3, the **dq** transition connects levels 3 and 1 in each manifold, i.e., at i, $m = 3$ and k, $n = 1$. The corresponding terms determining their amplitude in the (+ +) and (+ −) quadrants are $M_{33}M_{11}$* and $M_{13}M_{31}$*. In the limit of weak hyperfine coupling, the first product corresponds to two allowed transition amplitudes and the second to two forbidden ones with $\Delta m_I = \pm 2$. On the other hand, when the hyperfine interaction dominates the nuclear spin Hamiltonian, $M_{13}M_{31}$* contains the allowed transitions and $M_{33}M_{11}$* the forbidden transitions. Consequently, cross-peaks appear in the (+ +) quadrant for weak hyperfine and in the (+ −) quadrant for dominant hyperfine coupling.

HYSCORE spectra in Figure 2 simulated using eq 1 with the same parameters as Figure 1 confirm these quantitative considerations. For the large hyperfine coupling, $A = 5$ MHz, the **dq** correlations (1 and 1′ in the notation of Figure 1) produce narrow intense peaks with maximal frequencies in the (+ −) quadrant. Comparison of Figures 1 and 2 reveals that correlations ($\nu_{\mathbf{dq}\alpha}$, $\nu^{(1,2)}_{\mathbf{sq}\beta}$), ($\nu^{(1,2)}_{\mathbf{sq}\beta}$, $\nu_{\mathbf{dq}\alpha}$), i.e., (2, 3 and 2′, 3′), and ($\nu_{\mathbf{dq}\beta}$, $\nu^{(1,2)}_{\mathbf{sq}\alpha}$), ($\nu^{(1,2)}_{\mathbf{sq}\alpha}$, $\nu_{\mathbf{dq}\beta}$) (4, 7 and 4′, 7′) also contribute to the (+ −) quadrant. However, their peak intensities are lower than the intensity of **dq** correlations. Only the ($\nu^{(1,2)}_{\mathbf{sq}\beta}$, $\nu^{(1,2)}_{\mathbf{sq}\alpha}$) (5, 5′ and 9, 9′)

(15) (a) Muha, G. M. *J. Chem. Phys.* **1980**, *73*, 4139. (b) Muha, G. M. *J. Magn. Reson.* **1982**, *49*, 431. (c) Bowman, M. K.; Massoth, R. J. In *Electron Magnetic Resonance Applications of the Solid State*; Weil, J. A., Bowman, M. K., Morton, J. R., Preston, K. F., Eds.; CSC: Ottawa, 1987; p 99.

(16) Dikanov, S. A.; Bowman, M. K. *J. Magn. Reson., Ser. A* **1995**, *116*, 125.

(17) Dikanov, S. A.; Bowman, M. K. Manuscript in preparation.

(18) Flanagan, H. L.; Singel, D. J. *J. Chem. Phys.* **1987**, *87*, 5606.

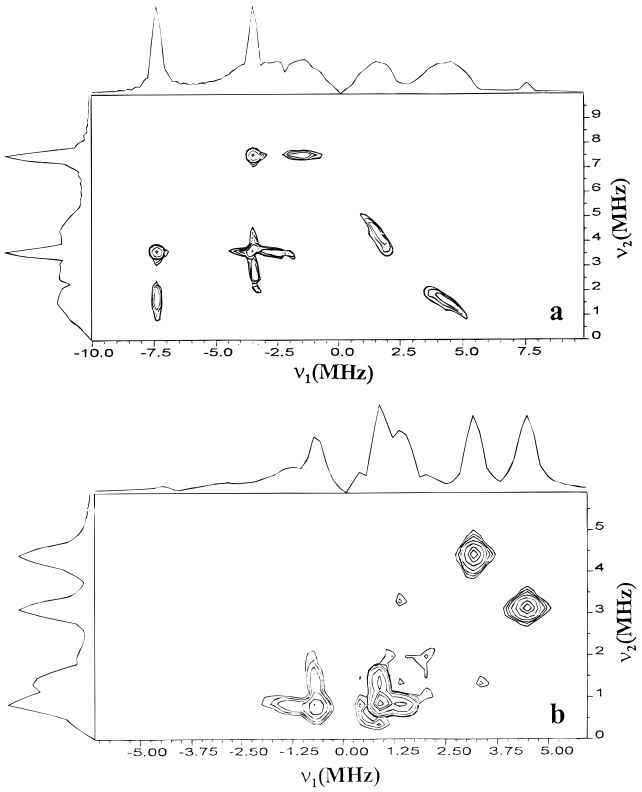

Figure 2. Simulated HYSCORE spectra at $A = 5$ MHz, $\nu_I = 1.08$ MHz, $K = 0.6$ MHz, $\eta = 0.5$, and $\tau = 136$ ns (a) and at $A = 1.1$ MHz, $\nu_I = 1.08$ MHz, $K = 0.81$ MHz, $\eta = 0.5$, and $\tau = 400$ ns (b).

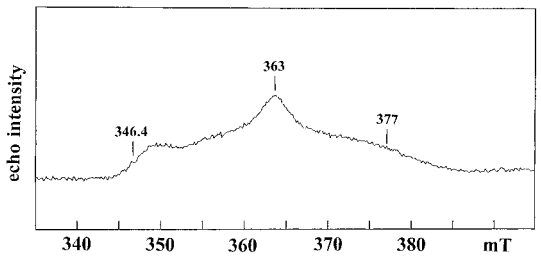

Figure 3. Field-sweep two-pulse ESE spectrum ($\tau = 240$ ns) of reduced 2,4,5-T monooxygenase. The microwave frequency was 9.72 GHz.

correlations appear in the (+ +) quadrant as follows from their characteristic orientation perpendicular to the diagonal. For weak hyperfine coupling of $A = 1.1$ MHz, the **dq** correlations (1 and 1′) produce peaks of maximal intensity in the (+ +) quadrant. There are also cross-ridges correlating $\nu^{(1)}_{\mathbf{sq}\beta}$ and $\nu^{(1)}_{\mathbf{sq}\alpha}$ (9 and 9′) which have comparable intensity in both quadrants.

In agreement with these results, the best resolved experimental HYSCORE spectra[13,19] show, in the case of strong hyperfine coupling, that the highest intensity occurs for those features correlating the **dq** transitions in the (+ −) quadrant and that spectral intensity is distributed rather uniformly along the other elongated cross-lines involving **sq** transitions. The **sq** cross-peaks, even with orientation selection, typically have much smaller peak intensities than the nearly isotropic **dq** peaks and in samples of frozen protein solutions may be observable only in 2D spectra with high signal to noise ratios.

Results

The field-swept two-pulse ESE spectrum of reduced 2,4,5-T monooxygenase, Figure 3, has an anisotropic line with a rhombic **g** tensor, $g_1 = 2.01$, $g_2 = 1.91$, $g_3 = 1.76$, whose principal values correspond to those of the CW EPR spectra.[9] Measurement of

(19) Dikanov, S. A.; Samoilova, R. I.; Smieja, J. A.; Bowman, M. K. *J. Am. Chem. Soc.* **1995**, *117*, 10579.

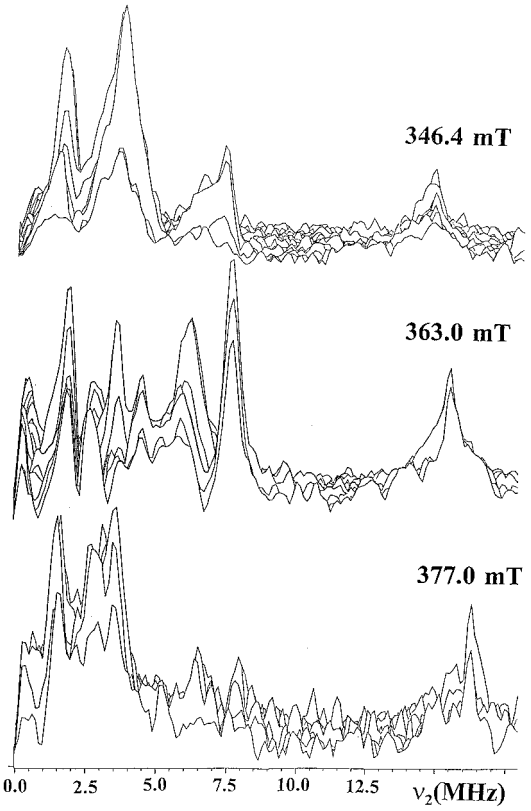

Figure 4. Superimposed plot of a set of three-pulse ESEEM spectra as the modulus of the Fourier transforms along the time τ axis recorded at the following points of the EPR spectrum: 346.4 mT ($g = 2.005$), 363 mT ($g = 1.913$), 377 mT ($g = 1.84$). The initial τ is 88 ns in the nearest trace, increased by 16 ns in the successive traces. The microwave frequency was 9.72 GHz.

echo envelopes at different points in the anisotropic EPR line selects iron−sulfur clusters with different orientations of the effective **g** tensor relative to the applied magnetic field. Ideally, the ESEEM spectra taken at the high and low extreme edges near the maximal and minimal g values give "single-crystal-like" patterns from those clusters whose g_1 and g_3 axes are directed along the magnetic field. In contrast, the resonance condition at the intermediate g_2 value is fulfilled by many different, yet well-defined, orientations.

Three-Pulse Spectra. Figure 4 shows stacked plots of three-pulse ESEEM spectra recorded as a function of time τ at the low- and high-field edges of the EPR spectrum and near the middle where the EPR intensity is maximum. They contain a peak near 15 MHz resulting from superhyperfine couplings of the unpaired electron spin with surrounding protons. In addition to the proton peak, a set of lines in the region 0−8 MHz are present in each stacked plot. The data in Figure 3 clearly indicate the orientational dependence of spectra obtained at different magnetic fields. At both edges, the intensity of the ESEEM frequencies in the region 5−8 MHz is significantly less than the intensity of lower frequency peaks. In contrast, in the central part the peaks at 5−8 MHz are comparable with those at low frequencies. The frequencies and number of intense peaks between 0 and 5 MHz vary. The positions of the two highest-frequency peaks change by about ∼0.5 MHz.

Spectra obtained in the $g_2 = 1.91$ (363 mT) region contain two intense peaks with maxima at 6.2 and 7.6 MHz (±0.05 MHz). These two frequencies are both significantly larger than the maximum modulation frequency of ∼4.5 MHz from peptide nitrogens observed in X-band ESEEM spectra of reduced ferredoxin clusters. This pair of high-frequency peaks are the

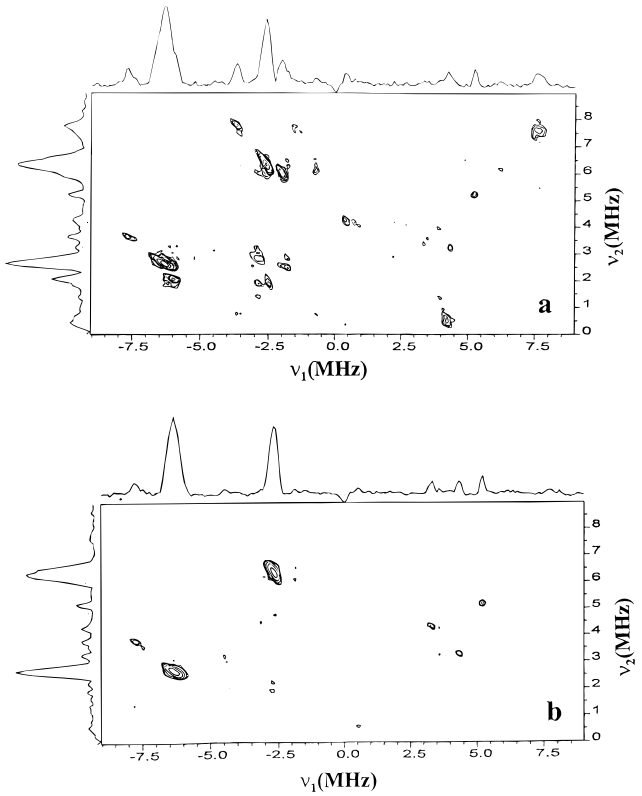

Figure 5. HYSCORE spectra of 2,4,5-T monooxygenase (τ = 136 ns) recorded at magnetic fields of 363 mT (g = 1.913) (a) and 359 mT (g = 1.934) (b). The microwave frequency was 9.72 GHz.

characteristic indication of Rieske clusters reported in all previous ESEEM studies.[5−7,9] They are assigned to **dq** transitions, $\nu_{\mathbf{dq}+}$, of two directly coordinated nitrogens from histidine residues with hyperfine couplings of ∼4 and ∼5 MHz. Theoretical considerations and numerical simulations[18] support the extensive experimental data,[20] indicating that both **dq** transitions from opposite electron spin manifolds have significant intensity for a nitrogen with a hyperfine coupling a few times larger than the nuclear Zeeman frequency. In previous investigations of Rieske clusters, two lines in the frequency region 2.5−4.0 MHz were reported as $\nu_{\mathbf{dq}-}$ transitions.

HYSCORE Spectra near g_2 = 1.91. Conclusive experimental observation of the pair of **dq** transitions for each nitrogen can be made from the HYSCORE spectrum (Figure 5a). The value of τ affects the intensities of the HYSCORE lines; however, this particular spectrum contains all resolved correlation features. The largest intensities belong to three pairs of cross-peaks with maxima at [±7.6, ∓3.6], [±6.4, ∓2.7], and [±6.0, ∓2.0] MHz in the (+ −) quadrant. We use the notation [±7.6, ∓3.6] MHz to denote the pair of cross-peaks with coordinates (+7.6, −3.6) and (+3.6, −7.6) MHz. The first two pairs with the largest coordinates confirm the previous assignment[9] of 6.4 and 2.7 MHz and 7.6 and 3.6 MHz lines in the one-dimensional spectrum in Figure 4 (363 mT) as pairs of **dq** transitions from two different histidine nitrogens with a smaller (N1) and a larger (N2), hyperfine coupling, respectively. The two peaks in the (+ +) quadrant with maxima at about [4.2, 0.5] MHz most likely correlate the larger and smaller **sq** transitions from two manifolds of the N1 nitrogen (however, below we discuss another possibility). The weak traces at (7.7, −1.5) and (6.2, −0.7) MHz correlate **dq** transitions with smaller **sq** transitions for both nitrogens. The peaks in the region [±(2.0−3.0), ∓(2.0−3.0)] MHz appear where lines correlating **sq** transitions are expected to cross. The sharp peaks at (5.3, 5.3) MHz and several others exactly along the diagonal in HYSCORE spectra are instrumental artifacts related to the pulse programmer clock.

The remaining strong features at [±6.0, ∓2.0] MHz are most notable. These peaks are present in all HYSCORE spectra recorded with τ between 104 and 272 ns at this magnetic field and are comparable in intensity with the cross-peaks at [±7.6, ∓3.6] and [±6.4, ∓2.7] MHz correlating **dq** transitions. Deviation of ∼2−3 mT from g_2 = 1.91 at τ = 136 ns leads to the disappearance of the [±6.0, ∓2.0] MHz peaks. A significant decrease of intensity but not complete disappearance takes place also for the peaks at [±7.6, ∓3.6] MHz. Figure 5b shows a HYSCORE spectrum obtained at the field 359 mT (g = 1.934) and τ = 136 ns. This spectrum, like the spectrum from 363 mT, still contains intense lines at [±6.4, ∓2.7] MHz, but other features in the (+ −) quadrant are no longer resolved except a weak peak at (−7.6, 3.6) MHz. An additional pair of correlations at [4.3, 3.2] MHz appears in the (+ +) quadrant, only one of which was seen in the spectrum at 363 mT.

The significant intensity of the [±6.0, ∓2.0] MHz peaks together with their line shape is typical of cross-peaks involving **dq** transitions, and it is tempting to assign them to a third set of **dq** transitions which in the 1D three-pulse spectra strongly overlap the lines at 6.4 and 2.7 MHz. In that case, they would indicate a third nitrogen with A = 3.5 MHz and $\kappa^2 = K^2(3 + \eta^2)$ = 0.78 MHz^2 (K = 0.47 ± 0.03 MHz).[21] Tsang et al.[22] reported unusual features in both the EXAFS and the XANES spectra of the reduced [2Fe-2S] Rieske cluster in phthalate dioxygenase from *B. cepacia* that could be interpreted as the binding of an additional low-Z ligand to the reduced cluster, giving one four-coordinated and one five-coordinated iron. Because the ENDOR data[3] showed coordination of only two nitrogens in reduced phthalate dioxygenase, Tsang et al. speculated that the most likely candidate for an additional ligand is an oxygen either from an amino acid side chain or from the peptide backbone. The observation of peaks in the 2D HYSCORE spectrum which might be assigned to a third nitrogen with hyperfine coupling very close to the couplings determined in ENDOR and 1D ESEEM spectra raises the possibility of coordination by a third side-chain nitrogen. However, this interpretation is incompatible with previous interpretations of experimental data for Rieske centers. In addition, these peaks are observed only near g = 1.91 and have a magnetic field dependence that is quite different from that of the two directly coordinated nitrogens. Simulations indicate that **dq** correlation peaks for a nitrogen with coupling near those predicted for a third strong nitrogen have appreciable intensity at most orientations. Consequently, it is unlikely that this pair of peaks correlate **dq** transitions of a third strongly coupled nitrogen, and we must carefully examine the assignment of these peaks.

The first possibility assigns these cross-peaks to two **sq** transitions of the N2 nitrogen. This gives two sets of N2 frequencies: 7.6, 6.0, and 1.6 MHz in one electron spin manifold, and 3.6, 2.0, and 1.6 MHz in the other. However, the quadrupole coupling of ∼2.3 MHz required by the first set of frequencies greatly exceeds the coupling required by the second set (∼0.2 MHz). Therefore, the assignment of these

(20) Dikanov, S. A.; Tsvetkov, Yu. D. *Electron Spin Echo Envelope Modulation (ESEEM) Spectroscopy*; CRC Press: Boca Raton, FL, 1992; Chapters 10 and 15.

(21) The coupling A and parameter κ of ^{14}N were calculated assuming the double-quantum frequencies 6.0 and 2.0 MHz from eq 5: Dikanov, S. A.; Tsvetkov, Yu. D.; Bowman, M. K.; Astashkin, A. V. *Chem. Phys. Lett.* **1982**, *90*, 149.

(22) Tsang, H.-T.; Batie, C. J.; Ballou, D. P.; Penner-Hahn, J. E. *Biochemistry* **1989**, *28*, 7233.

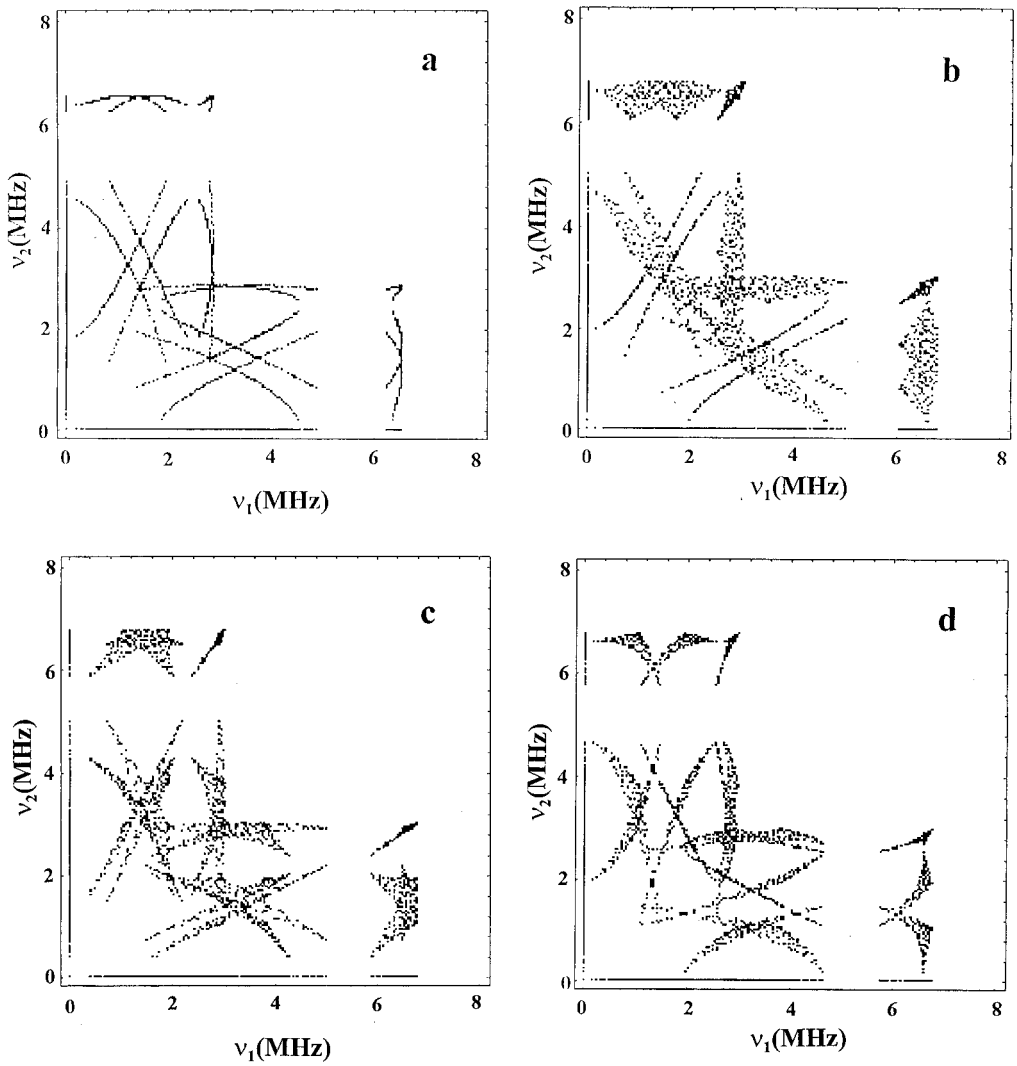

Figure 6. Contour line shape of the cross-peaks from the nitrogen ^{14}N, $\nu_I = 1.08$ MHz, $K = 0.6$ MHz, and $\eta = 0.5$ (quadrupole tensor −1.2, 0.9, 0.3 MHz), for isotropic hyperfine coupling $a = 4.0$ MHz (a) and anisotropic hyperfine with principal axes coincident with the quadrupole tensors (b) 4.25, 4.25, 3.5 MHz, (c) 4.25, 3.5, 4.25 MHz, and (d) 3.5, 4.25, 4.25 MHz.

peaks as a **sq** correlation for N2 is excluded. Similar considerations preclude the interpretation of these peaks as correlations between **sq** frequencies of the N1 nitrogen.

The other interpretation considers these intense peaks at [±6.0, ∓2.0] MHz as a **dq**−**sq** correlation of the N2. A second correlation of this type may be found in weak trace (6.1, −0.7) MHz. Then the set of N2 nuclear frequencies would be 2.7, 2.0, and 0.7 MHz. With such a choice of frequencies one may suggest that the (4.2, 0.5) MHz features from the (+ +) quadrant correlate the low frequency from this set with the larger **sq** frequency from the other manifold containing 6.3, 4.2, and 2.1 MHz. These sets of frequencies lead to the reasonable estimation of the quadrupole couplings of ∼0.4−0.7 MHz. Thus, we have an internally consistent interpretation of the [±6.0, ∓2.0] MHz peaks as a **dq**−**sq** correlation with the additional assignment of the (4.2, 0.5) and (6.1, −0.7) MHz features to the same nitrogen. Yet this interpretation contradicts the weak intensity for these peaks in all reported HYSCORE spectra with intense **dq** correlations in the (+ −) quadrant.[13,19]

Our interpretation is supported by simulations of contour line shape and HYSCORE spectra. Introduction of the anisotropic hyperfine changes the contour line shape of cross-features to patches instead of arcs (Figure 6, the parameters used in the simulations are based on the estimation discussed in Comparison with Benzene Oxygenase). The shape of these areas is very sensitive to the relative orientation of the nitrogen quadrupole and hyperfine tensors. For the **dq**−**dq** features, hyperfine anisotropy lengthens and bends the cross-peaks which remain rather narrow. The **dq**−**sq** correlations acquire a "butterfly shape". The two wings may overlap or be separated. Also their areas depend on the relative orientation of nitrogen hyperfine and quadrupole tensor and may become comparable in area to that of the **dq**−**dq** transitions in some cases.

For certain orientations of **g**, hyperfine, and quadrupole tensors one of the **sq** transitions can be nearly constant in frequency for those orientations selected at a special magnetic field. This can produce a relatively sharp, strong **sq**−**dq** correlation feature appearing at a very restricted range of the EPR spectrum. We have observed the qualitative indications of such a phenomenon in model orientationally-selected simulations of HYSCORE spectra.

However, final confirmation of this interpretation for the [±6.0, ∓2.0] MHz peaks requires a multifrequency experiment leading to changes in the peak positions with variations in the microwave frequency or selective isotopic substitution of the histidine nitrogens.

Special attention is called to the peaks [4.2, 3.3] MHz which appear in the spectra of Figure 5 in the (+ +) quadrant along with the [4.2, 0.5] MHz peaks. Earlier, we noted the [4.2, 0.5] MHz peaks were consistent with assignment as correlation features of N2. However, the [4.2, 3.3] MHz feature definitely does not belong to that same nitrogen, because 3.3 MHz exceeds

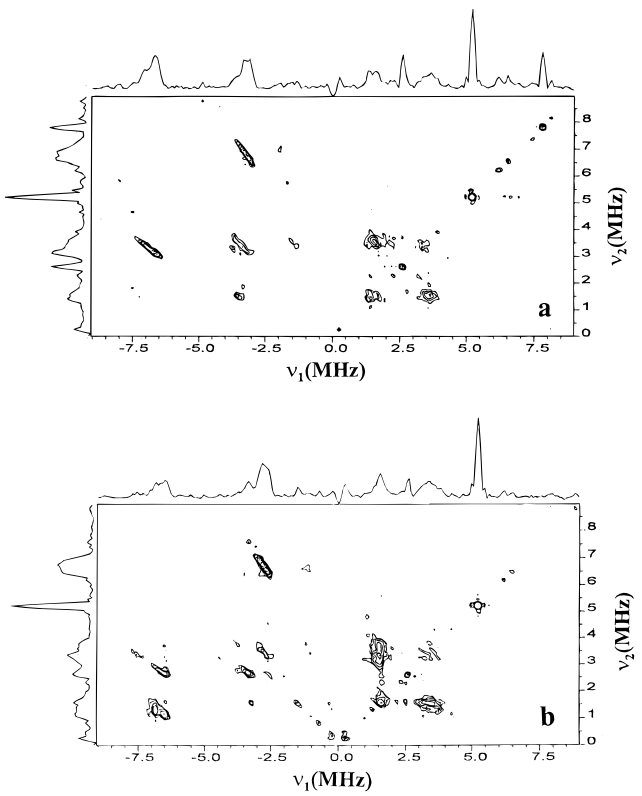

Figure 7. HYSCORE spectra of 2,4,5-T monooxygenase recorded at magnetic fields of 346.4 mT ($g = 2.005$, $\tau = 112$ ns) (a) and 377 mT ($g = 1.84$, $\tau = 104$ ns) (b). The microwave frequency was 9.72 GHz.

the frequency of the **dq** transition, 2.6 MHz, of N2. The possibility that [4.2, 3.3] MHz correlates **sq** transitions of N1 leads to the sets of frequencies 7.7, 4.2, and 3.3 MHz and 3.6, 3.3, and 0.3 MHz which are internally inconsistent. Thus, the [4.2, 3.3] MHz lines cannot arise from one of the histidine nitrogens, and we assign it below to a peptide nitrogen.

HYSCORE Spectra at Other Fields. It is very difficult to reliably recognize the $\nu_{\mathbf{dq}-}$ peaks in stacked plots of three-pulse ESEEM spectra (Figure 4) obtained near the turning points of the EPR spectrum due to spectral congestion and overlap of lines. In contrast, the HYSCORE spectra (Figure 7) clearly indicate the pairs of **dq** transitions for both nitrogens: 2.95 and 6.5 MHz (N1), 3.4 and 7.15 MHz (N2) at the low-field edge, and 2.7 and 6.6 MHz (N1), 3.4 and 7.6 MHz (N2) at the high-field edge. The cross-peaks in the low-field spectrum strongly overlap, but the larger **dq** frequencies are known from three-pulse spectra, and careful analysis of the contour HYSCORE spectra and its skyline projections on both axes reveal the contribution of two features in the corresponding cross-peaks.

The peak at (−6.6, 1.1) MHz and the pair at [±3.5, ∓2.7] MHz, together with the stretched ridges [∼3.6, ∼1.5] MHz in the spectrum at 377 mT allow us to reconstruct the two sets of N1 nuclear frequencies as 6.6, 3.6, and 3.0 MHz and 2.7, 1.5, and 1.2 MHz. The [3.6, 1.5] MHz peaks together with the **dq** correlations dominate the (+ +) quadrant of the spectrum at 346.4 mT. These transitions produce the weak traces in the (+ −) quadrant also. They definitely belong to features correlating the **sq** transitions. The assumption that they are produced by N1 leads to nuclear frequencies at this field of 6.5, 3.6, and 2.9 MHz and 2.95, 1.5, and 1.45 MHz. However, second-order estimates[23] of the diagonal components of the quadrupole tensor in the **g** tensor coordinate system based on N1 frequencies constructed from HYSCORE spectra recorded near the canonical orientations yield a nonphysical tensor with significant nonzero trace. This problem may result from incorrect assignment of some weak peaks in Figures 5 and 7 or from a breakdown of the assumption of strong hyperfine coupling for N1 with $A \approx 3.5-4$ MHz.

The HYSCORE spectra provide important information about the correlations between the different ESEEM frequencies beyond that obtainable from 1D spectroscopies. However, the large number of overlapped features of weak intensity from even one $I = 1$ nucleus can still present the difficulties for their complete interpretation. In such situations, the selective isotope substitution as was done for the Rieske center in phthalate dioxygenase[3] would be a powerful adjunct for complete determination of hyperfine and quadrupole tensors.

Comparison with Benzene Dioxygenase. Previous ESEEM studies of Rieske centers focused on those similarities between the spectra of different proteins indicating coordination by two histidine nitrogens. Therefore, it is interesting to compare the data discussed above with the only available set of similar data (stacked plots of three-pulse spectra and a HYSCORE spectrum near $g_2 = 1.91$) for benzene dioxygenase from *P. putida* recently published by Shergill et al.[7] with the aim of estimating the sensitivity of ESEEM to minor differences in the environment of the Rieske cluster.

The three-pulse ESEEM spectra recorded[7] by Shergill et al. at $g_2 = 1.91$ contain six lines at ∼1.8, 2.6, 3.2, 4.5, 6.1, and 7.5 MHz which are in close agreement with the frequencies 2.0, 2.9, 3.4, 4.5, 6.3, and 7.6 MHz in the spectrum in Figure 3 (363 mT). Only one additional peak of intermediate intensity at ∼0.5 MHz is present in our spectrum. Although the frequencies for both proteins are very similar, their relative peak intensities are significantly different. The peak at 7.6 MHz dominates the spectrum of the benzene dioxygenase and is at least twice as intense as any other line. In contrast, the four peaks at 2.0, 3.4, 6.3, and 7.6 MHz differ by ∼25% in intensity in the profile of the three-pulse ESEEM spectra of 2,4,5-T monooxygenase.

The HYSCORE spectrum of benzene dioxygenase[7] contains three pairs of peaks near each other in the (+ −) quadrant: [±7.2, ∓3.2], [±6.5, ∓2.7], and [±6.3, ∓1.8] MHz. The first two pairs of peaks are the **dq** correlations for two-coordinated histidine nitrogens and are similar to the pairs of peaks at [±7.6, ∓3.6] and [±6.4, ∓2.7] MHz in the spectrum on Figure 5a. A problem arises in the interpretation of the peaks at [±6.3, ∓1.8] MHz which have characteristics similar to those of the peaks at [±6.0, ∓2.0] MHz in our spectra. All of our previous discussion related to the cross-peaks at [±6.0, ∓2.0] MHz also applies to the peaks at [±6.3, ∓1.8] MHz. The observation of these peaks in the spectra of both proteins as well as the overall similarity of the spectra emphasizes the basic structural similarities shared by two Rieske centers, even down to the peaks near [±6.0−6.3, ∓1.8−2.0] MHz that were missed by one-dimensional spectroscopies. Additionally, three pairs of peaks with weaker intensities correlating the **sq**−**sq** or **sq**−**dq** features in the (+ −) quadrant are seen by Shergill et al.[7] They do not, however, coincide with the low-intensity peaks of corresponding features in our spectra. Further, the (+ +) quadrant in the spectrum of Shergill et al.[7] contains only the cross-peaks [∼4.0, 2.6] MHz in contrast to the [4.2, 0.5] and [4.2, 3.3] MHz peaks in 2,4,5-T monooxygenase.

In short, the HYSCORE spectra of both proteins show three types of cross-peaks: two pairs of double-quantum correlations from the two ligated histidine nitrogens, an additional pair of intense peaks presently attributed to a **dq**−**sq** correlation of N1, and several weak cross-peaks. However, there are small but systematic differences in the frequencies of all the cross-features and in the derived magnetic tensors of the two proteins.

Table 1. Diagonal Components of the Nitrogen Hyperfine Tensors (MHz) in the g Tensor Coordinate System of the Reduced Rieske Centers

	nitrogen 1				nitrogen 2				
protein	A_1	A_2	A_3	a	A_1	A_2	A_3	a	ref
2,4,5-T monooxygenase from *B. cepacia*	4.05	3.88	4.01	3.98	4.71	5.07	5.02	4.93	this work
benzene dioxygenase from *P. putida*[a]	3.47	3.56	3.95	3.66	4.49	4.96	4.94	4.79	Shergill et al.[7]
phthalate dioxygenase from *B. cepacia*[b]	4.10	3.85	4.86	4.27	5.98	5.00	5.56	5.51	Gurbiel et al.[3]

[a] The diagonal components were recalculated using the values A and e^2qQ/h determined with eq 5 at different points of the EPR spectrum. [b] The diagonal components were recalculated using the principal values of hyperfine tensors and the Euler angles of their orientations relative to the **g** tensor axes.

Shergill et al.[7] estimated hyperfine and quadrupole couplings at points in the EPR spectra near the principal directions of the **g** tensor on the basis of the expression for the maximum value of the **dq** frequency,

$$\nu_{\mathbf{dq}\alpha(\beta)} = 2[(\nu_I \pm A/2)^2 + \kappa^2]^{1/2} \quad (5)$$

originally obtained from the graphical analysis of the orientational dependence of nitrogen nuclear frequencies in the case of isotropic hyperfine coupling.[21] The application of this formula for the two **dq** transitions gives the following values of A, 3.36, 3.50, and 3.82 MHz (N1) and 4.44, 4.99, and 4.92 MHz (N2), and κ, 0.98, 1.11, and 1.25 MHz (N1) and 0.98, 1.05, and 1.07 MHz (N2) for the low-, middle-, and high-field parts of the iron−sulfur cluster EPR spectrum of benzene dioxygenase, respectively.

We have extended the approach developed to derive eq 5 to the case of arbitrary hyperfine interaction. We find the maximum frequency of the **dq** transition is

$$\nu_{\mathbf{dq}\alpha(\beta)} = 2[\nu_{\alpha(\beta)}{}^2 + \kappa^2]^{1/2} \quad (6)$$

where $\nu_{\alpha(\beta)}{}^2 = \sin^2\theta\cos^2\phi\,(\nu_I \pm A_X/2)^2 + \sin^2\theta\sin^2\phi\,(\nu_I \pm A_Y/2)^2 + \cos^2\theta\,(\nu_I \pm A_Z/2)^2$. A_X, A_Y, and A_Z are the principal values of the hyperfine tensor, and θ and ϕ determine the orientation of the magnetic field in the principal axis system of the hyperfine tensor. Equation 6 shows that Shergill et al. actually estimated

$$A_{\text{eff}} = (\nu_{\mathbf{dq}\alpha}{}^2 - \nu_{\mathbf{dq}\beta}{}^2)/8\nu_I = \sin^2\theta\cos^2\phi\,A_X + \sin^2\theta\sin^2\phi\,A_Y + \cos^2\theta\,A_Z \quad (7)$$

near the canonical orientations of the **g** tensor, with the different angles θ and ϕ giving the orientation of the principal g axes. The maximum **dq** frequency thus has the same dependence on the quadrupole interaction for either isotropic or anisotropic hyperfine and is independent of the relative orientation of quadrupole and hyperfine tensors.

This estimation should yield the same value of κ at all orientations. The significant spread in reported κ may indicate that the **dq** frequencies did not reach their maximum values at all field values due to orientation selection, or that the peak positions could not be determined with sufficient accuracy in three-pulse spectra due to overlap.

Application of eq 6 to the three pairs of **dq** transitions measured from HYSCORE spectra at both extreme edges and at the middle of the EPR spectrum of 2,4,5-T monooxygenase gives A_{eff}, 3.94, 3.77, and 3.91 MHz (N1) and 4.64, 5.01, and 5.05 MHz (N2), and κ, 1.16, 1.11, and 1.09 MHz (N1) (K = 0.6 ± 0.1 MHz) and 1.15, 1.15, and 1.06 MHz (N2) (K = 0.58 ± 0.1 MHz). The HYSCORE spectra allow more accurate measurement of the **dq** frequencies, helping to reduce the spread of κ.

There is an alternative way to use the available pairs of **dq** transitions at both extreme edges and at the middle of the EPR spectrum to estimate the diagonal elements of the nitrogen hyperfine tensor A_i in the **g** tensor coordinate system (i indexes the **g** tensor principal axes) from second-order expressions for the $\nu_{\mathbf{dq}\pm}$ frequencies as[23]

$$A_i = 2\nu_I(\nu_{\mathbf{dq}\alpha} + \nu_{\mathbf{dq}\beta})/[8\nu_I - (\nu_{\mathbf{dq}\alpha} - \nu_{\mathbf{dq}\beta})] \quad (8)$$

where $\nu_{\mathbf{dq}\alpha(\beta)}$ are taken from the corresponding spectrum obtained near g_i. This estimation gives a better description of the hyperfine anisotropy because eq 8 is valid for all **dq** frequencies measured in the experimental spectra rather than its maximum possible value. The A_i values estimated by this procedure can be described in terms of the principal values of the hyperfine tensor using the Euler angles relating the hyperfine tensor orientation to the **g** tensor. However, the sets of A_{eff} and A_i values obtained by these two methods are not significantly different, reflecting the low anisotropy of the histidine nitrogen hyperfine interaction.

The hyperfine elements found for 2,4,5-T monooxygenase are given in Table 1 together with those calculated using data for the reduced Rieske centers in benzene dioxygenase from *P. putida*[7] and phthalate dioxygenase from *B. cepacia*.[3] Comparison of data for these three proteins reveals a spread in isotropic couplings for both nitrogens and even larger differences in some of the diagonal components that reflect the differences in Fe−N ligation of each particular protein, leading to different orientations of the nitrogen hyperfine and quadrupole tensors relative to the **g** tensors axes and to different principal values.

Thus, ESEEM and particularly HYSCORE spectroscopies are sensitive to minor differences between these proteins including variations in the ligation geometry of both histidine nitrogens and in the nitrogens of the other amino acids.

Contribution of a Peptide Nitrogen to HYSCORE Spectra. Shergill et al.[7] report the contribution of a peptide nitrogen to the ESEEM spectra of the Rieske center in benzene dioxygenase in addition to the two histidine ligands.

Peptide nitrogens around a reduced [2Fe-2S] cluster with four cysteine ligands produce strong lines in three-pulse ESEEM spectra recorded near the point of the maximum EPR signal with frequencies 0.8−1.2, 1.9−2.1, 2.9−3.1, and 4.0−4.4 MHz.[8] Figure 8 shows the HYSCORE spectrum of such a cluster in the ferredoxin from *Porphira umbilicalis* which has a typical one-dimensional ESEEM spectrum produced by peptide nitrogens.[8f] The HYSCORE spectrum shows intense cross-peaks in the (+ +) quadrant at [3.9−4.3, 3.0−3.2] MHz correlating the **dq** with the largest quadrupole transition in opposite electron spin manifolds. Two peaks, [4.3, 3.0] and [3.9, 3.1] MHz, can be resolved in these ridges that are in agreement with recent C-band experiments showing interactions with at least two peptide nitrogens with different hyperfine couplings.[8f] The spectrum also shows intense peaks in the (+ −) quadrant from the lowest quadrupole frequency with a **sq** transition from the same manifold as the 3.9−4.3 MHz feature.

(23) Dikanov, S. A.; Tyryshkin, A. M.; Hüttermann, J.; Bogumil, R.; Witzel, H. *J. Am. Chem. Soc.* **1995**, *117*, 4976.

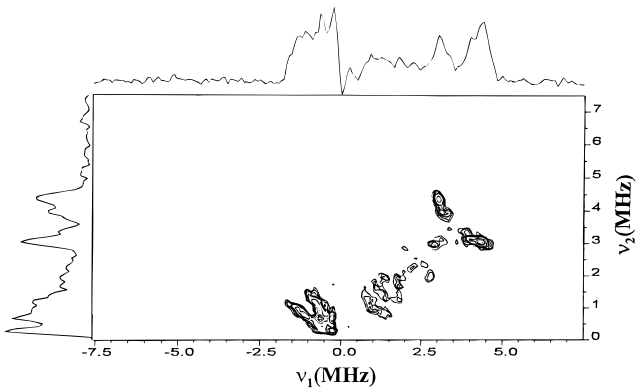

Figure 8. HYSCORE spectrum of reduced ferredoxin from *P. umbilicalis* recorded at a magnetic field of 355 mT and $\tau = 400$ ns. The ferredoxin in tris/D_2O buffer (0.5 M, pH 7.5) was reduced by dithionite in anaerobic conditions.

The assignment by Shergill et al. is mainly based on the 1.8 and 4.5 MHz peaks in the three-pulse spectra. However, this assignment is not supported by their HYSCORE spectrum. The frequency of 1.8 MHz is correlated with the frequency of 6.3 MHz by two intense peaks in the $(+\,-)$ quadrant and, therefore, must belong to the same manifold as the **dq** frequency of ~4.5 MHz unless there is an accidental degeneracy. Stronger evidence for the contribution of peptide nitrogen(s), in our view, comes from the weak peaks, [~4.0, 2.5] MHz, contributing to the $(+\,+)$ quadrant whose origin was not discussed.[7] These peaks are located close to the area of the $(+\,+)$ quadrant where peptide nitrogens appear in Figure 8. The narrow lines, [4.3, 3.3] MHz, in our spectra in Figure 5 also lie in the same area. Taken together, these data may indicate an additional structural motif involving peptide nitrogen(s) surrounding the Rieske-type cluster. The apparently weaker intensity for these peaks in the Rieske-type center compared to the plant ferredoxin cluster occurs because the dominant contribution to the ESEEM in the Rieske-type center arises from the directly ligated nitrogens which dwarf peaks from the peptide nitrogen involved in hydrogen bonding with the cysteine sulfur near the reduced iron atom.[8f] Comparison of these peptide peaks shows observable but minor variations of their frequencies in these three proteins determined mainly by variations in the strong quadrupole coupling of the peptide nitrogen ($K \approx 0.8$ MHz) and not in the hyperfine.

Our spectrum in Figure 5a contains additional peaks at [4.2, 0.5] MHz in the $(+\,+)$ quadrant. These can be interpreted as **sq** correlations. However, there is no compelling evidence for such an assignment because these frequencies are not involved in other correlations. They could equally well be a part of ridges correlating the **dq** peak of the peptide nitrogen with the smallest quadrupole frequency appearing only at the selected orientations.

Neither the previously reported ENDOR and ESEEM results nor our data including HYSCORE spectra give any evidence of a contribution from the remote nitrogens of the histidine residues. The data available for Cu^{2+} [24,25] and VO^{2+} [19,26] complexes with imidazole and Cu^{2+}−proteins[27] indicate that the ratio of hyperfine couplings of coordinated and remote nitrogens in the imidazole ring is about 20. This means that hyperfine couplings with remote nitrogens of the histidine ligands in the Rieske center should not exeed a few tenths of a megahertz. Therefore, X-band experiments are performed very far from the favorable cancellation condition[17] that produces narrow intense peaks in ESEEM spectra. The best way to detect these nuclei is through substitution of ^{14}N by ^{15}N.[19,26]

Conclusion

This study of the reduced Rieske cluster in 2,4,5-trichlorophenoxyacetate monooxygenase from *B. cepacia* AC1100 shows that HYSCORE spectroscopy is a very useful tool to correlate lines produced by the same nucleus in complex ESEEM spectra. The most pronounced and easily recognized features in HYSCORE spectra correlate **dq** transitions from opposite electron spin manifolds of each nuclei. Their assignment allows immediate estimation of the diagonal components of the hyperfine tensor in the **g** tensor coordinate system.

The HYSCORE spectra clearly show minor differences between proteins. Comparison with other available published results indicates that the Rieske-type cluster in 2,4,5-T monooxygenase differs in the principal values and the tensor orientations of its coordinated histidine nitrogens. The HYSCORE spectra also contain peaks from interactions with peptide nitrogens which were observed in HYSCORE spectra of the Rieske cluster in benzene dioxygenase. These differences might reflect slight variations of the nitrogen cluster structure responsible for the variations of their redox potentials. Previously,[8f] the lines observed in ESEEM spectra of plant ferredoxins were assigned to a peptide nitrogen of a particular amino acid residue hydrogen bonded to a cysteine sulfur. Apparently similar hydrogen bonds to cysteine sulfur occur in Rieske centers. Changes in those hydrogen bonds that control redox potential would also change hyperfine and quadrupole interactions, thus providing a means to test this possible mechanism for control of redox properties. Such experiments will require extensive isotopic substitution and multifrequency HYSCORE measurements.

We find a major difference in the isotropic hyperfine couplings of the directly ligated nitrogens in the two histidines coordinated to the iron of the Rieske center. Despite the apparent equivalence of the two nitrogens, the local protein structure consistently produces distinctly different hyperfine couplings. The estimated diagonal elements of the anisotropic hyperfine coupling in the **g** tensor axis system are quite different for each oxygenase. It is not yet clear to what extent such changes are due to changes in hyperfine principal value or to a rotation of the principal axes. Although the HYSCORE spectra have raised a number of intriguing possibilities in the relation of structure and function in the Rieske centers in oxygenases, it is clear that the there oxygenases examined to date are an insufficient number to establish a correlation and that additional oxygenases must be examined.

Acknowledgment. This work was sponsored by the U.S. Department of Energy under Contract DE-AC06-76 RLO 1830 and by Associated Western Universities, Inc., Northwest Division (AWU NW), under Grant DE-FG06-89 ER-75522 or DE-FG06-92RL-12451 with the U.S. Department of Energy. S.A.D. acknowledges the receipt of a Faculty Fellowship from the AWU NW. The authors are indebted to Professor R. Cammack for the communication of his article (ref 7) prior to publication.

JA960781X

(24) Sholl, H.-J.; Hüttermann, J. *J. Phys. Chem.* **1992**, *96*, 9684.
(25) Mims, W. B.; Peisach, J. *J. Chem. Phys.* **1978**, *69*, 4921.
(26) Dikanov, S. A.; Burgard, C.; Hüttermann, J. *Chem. Phys. Lett.* **1993**, *212*, 493.
(27) Mims, W. B.; Peisach, J. In *Advanced EPR. Applications in Biology and Biochemistry*; Hoff, A. J., Ed.; Elsevier: Amsterdam, 1989; p 1.